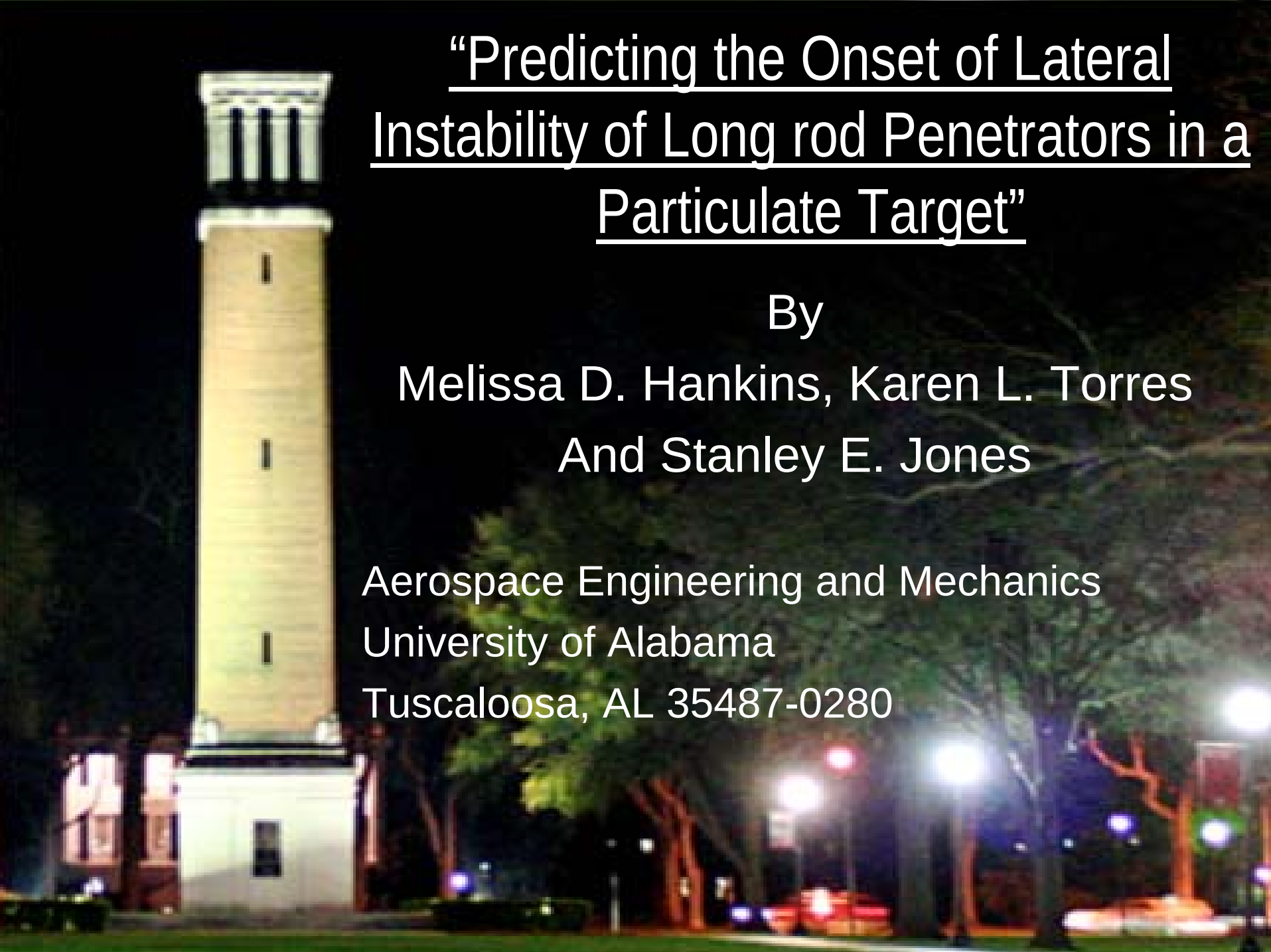

"Predicting the Onset of Lateral Instability of Long rod Penetrators in a Particulate Target"

By

Melissa D. Hankins, Karen L. Torres

And Stanley E. Jones

Aerospace Engineering and Mechanics

University of Alabama

Tuscaloosa, AL 35487-0280

Topics

- The Instability Problem
- Laboratory Scale Testing
- Normal Penetration of Particulate Targets
- Formulation and Solution of the Problem
- Results
- Conclusions and Future Work

The Instability Problem

Penetrator Material: High Strength Steel
Penetrator Material: 12.7 mm
Target: Remolded Eglin Sand
Impact Velocity: 1525 m/sec

Penetrator Material: 6061-T6 Aluminum
Penetrator Material: 4.17 mm
Target: Alumina Powder
Impact Velocity: 696 m/sec

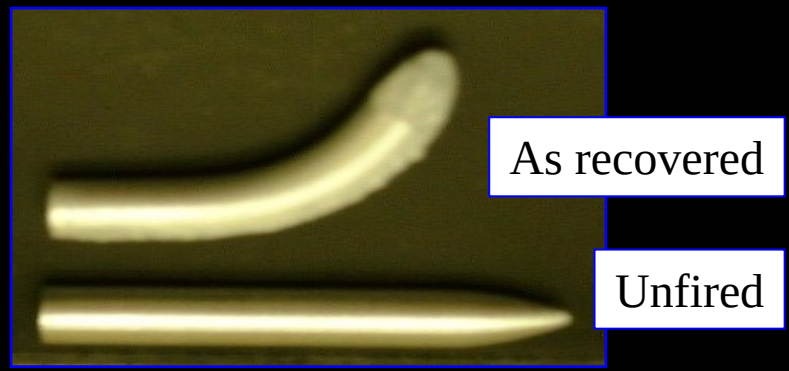

Experimental Data:

University of Alabama Ballistics Facility

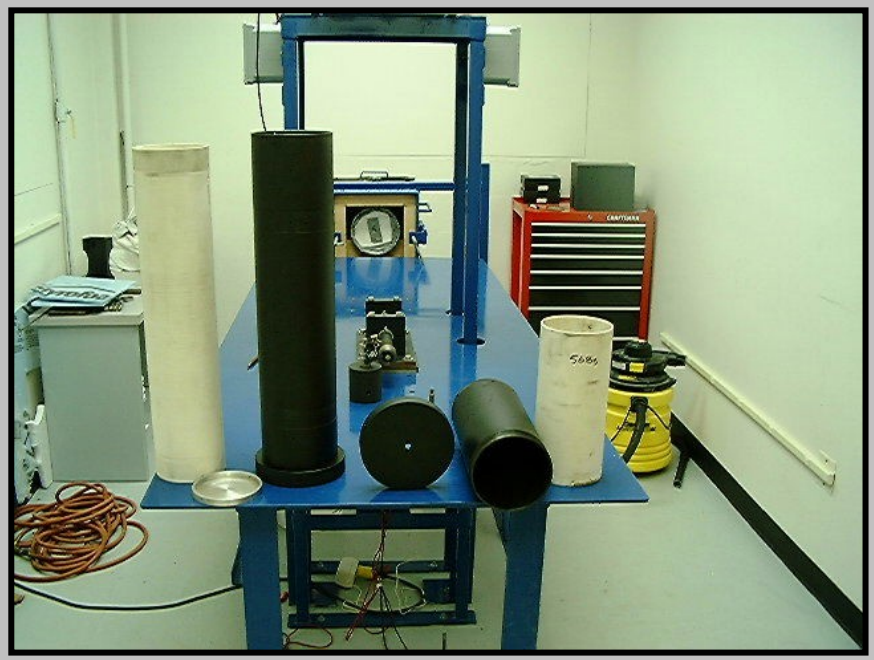

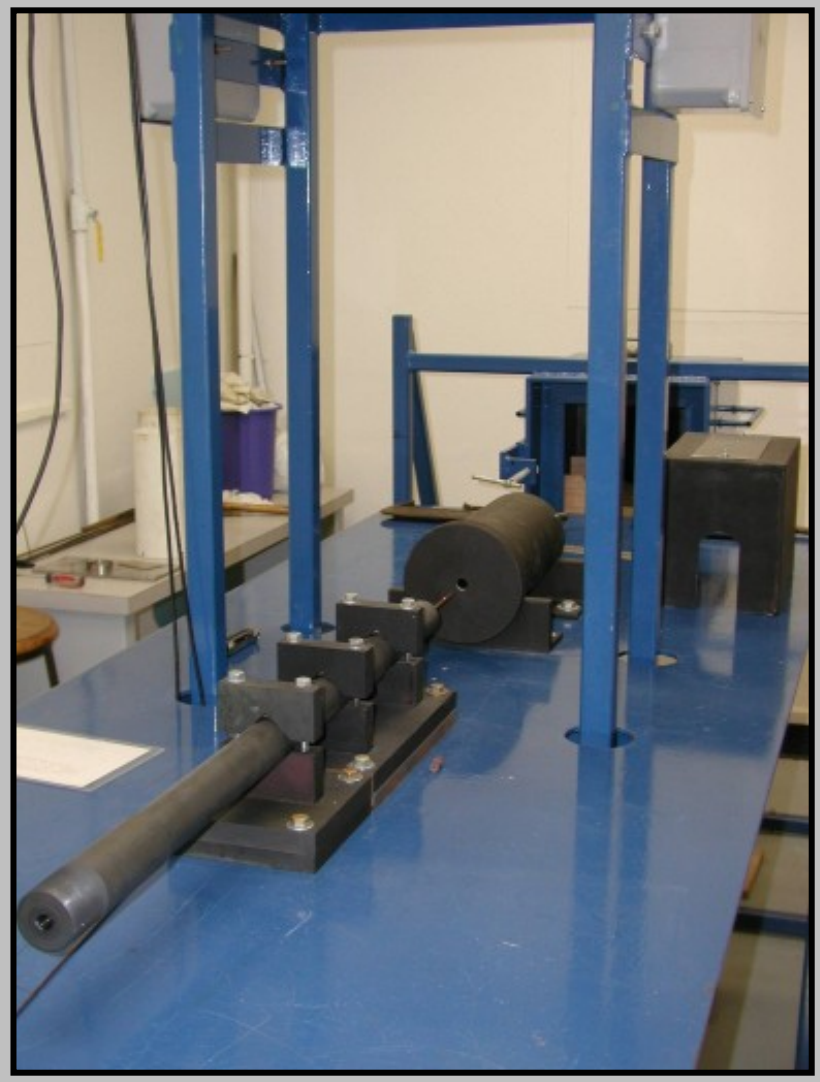

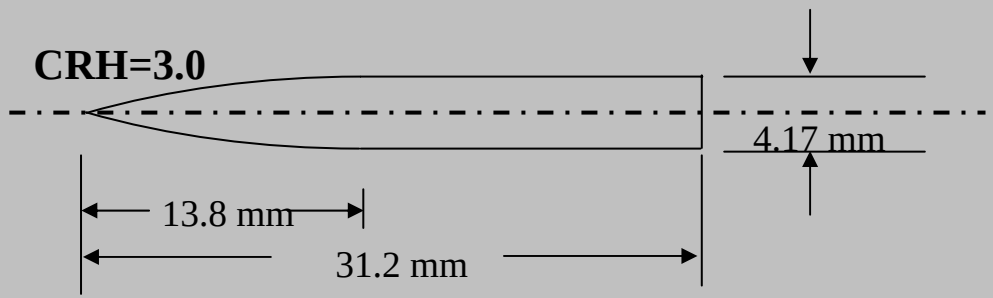

Schematic of Laboratory Penetration Test

1. **Steel target canister**
2. **Steel target face**
3. **Smooth-bore gun tube (167 caliber, 0.167 inch inside diameter bore)**
4. **Breech**
5. **Solenoid driver**
6. **Target sleeve in canister**
7. **Class 3A laser heads**
8. **Lenses which focus the laser beams on the projectile flight path**
9. **Receiving unit for laser beams with photomultiplier tubes**
10. **Small riser to prevent target material from spilling onto the photomultiplier tubes**

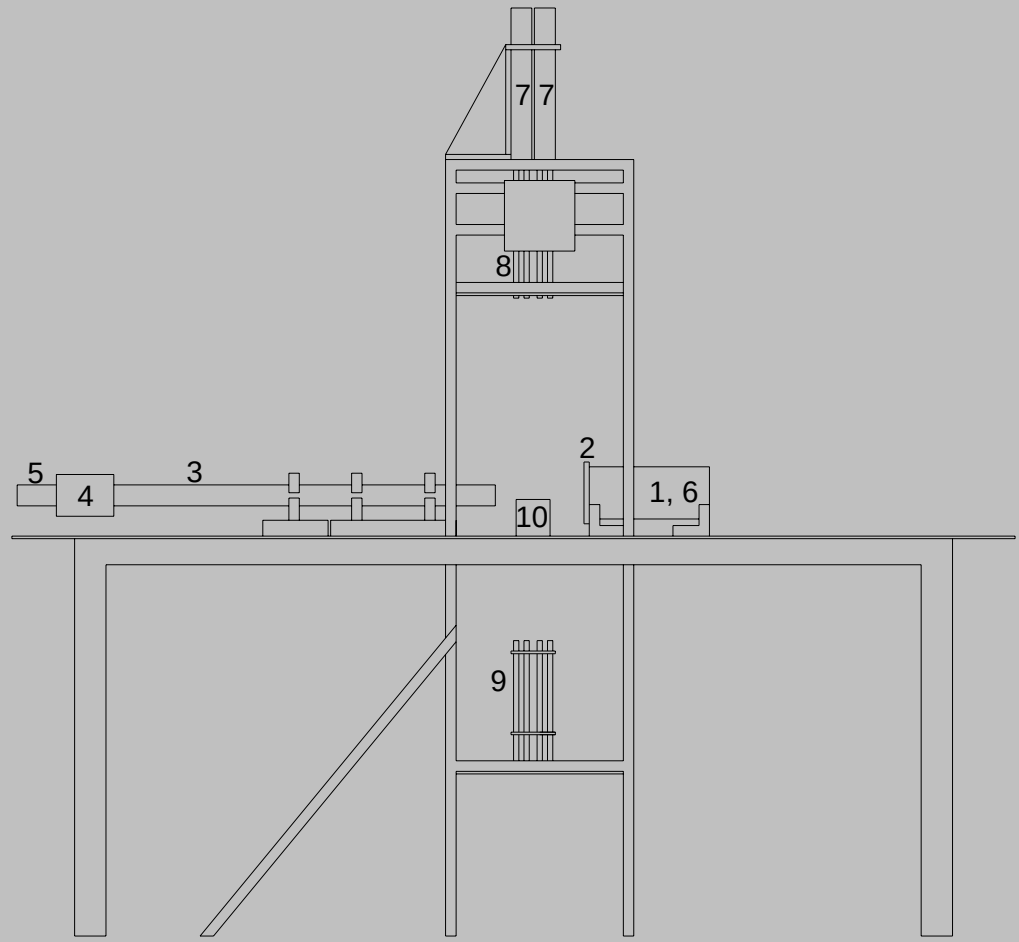

Laboratory Scale Penetration Testing

7075-T6 20:1Cylindrical Projectiles in Coarse Foundry Sand

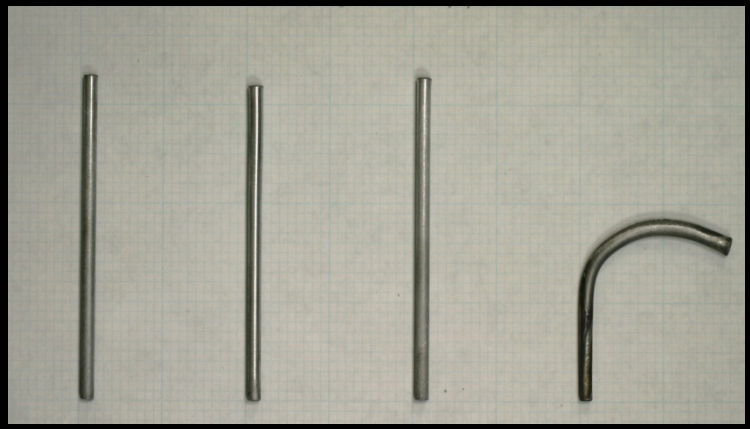

508 m/s 543 m/s 564 m/s 664 m/s

These figures demonstrate the progression of failure occurring after the critical velocity.

6061-T6 CRH 3.0 20:1 Projectiles in Coarse Foundry Sand

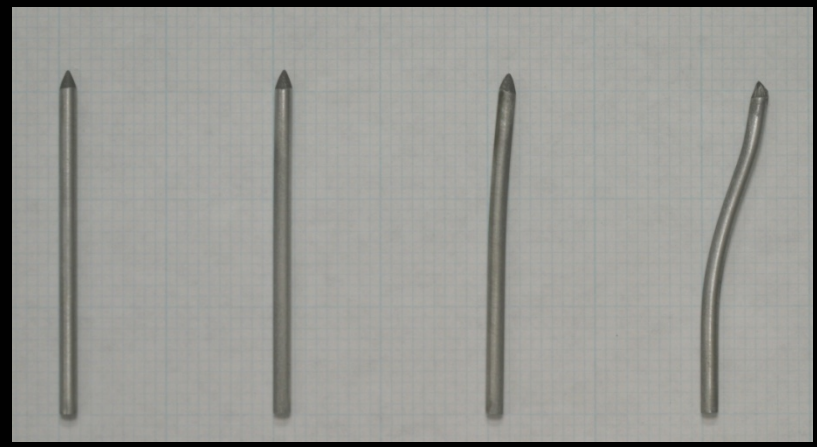

475 m/s 513 m/s 574 m/s 639 m/s

Normal Penetration Into Sand

$$P = \gamma \rho_t v_n^2 + R$$ (Pressure)

$$f = \mu P$$ (Friction)

Neglecting friction on the penetrator nose, the total penetration depth >L is

Normal Penetration Into Sand

$$z_f = L + \frac{1}{k}\ell n\left[\frac{e^{-kL_0}\left(v_0^2 + \frac{2\pi a^2 R}{mk} - \frac{4\pi\mu R a}{mk^2}\right) + \frac{4\pi\mu R a}{mk^2}}{\frac{2\pi a^2 R}{mk} + \frac{4\pi\mu R a L_0}{mk}}\right]$$

L = overall penetrator length

L_0 = shank length

$$k = \frac{2\pi a^2 \gamma \rho_t N}{m}$$

$$N = \frac{2}{a^2}\int_0^b \frac{rr'^3}{1+r'^2}dx$$

a= shank radius

b= nose length

μ= friction coefficient

R= target strength factor

m= penetrator mass

p_1= target density

Y= dimensionless drag coefficient

EVALUATION of γ

$$\gamma = \gamma_0 + \gamma_1\left(\frac{1}{N}\right) + \gamma_2\left(\frac{1}{N^2}\right) + \ldots$$

$\gamma = \gamma_0 + \gamma_1\left(\frac{1}{N}\right) + \gamma_2\left(\frac{1}{N^2}\right) + \gamma_3\left(\frac{1}{N^3}\right)$				
	γ_0	γ_1	γ_2	γ_3
Coarse Foundry Sand	0.660	0.397	0.140	0
Fine Foundry Sand	0.500	0.630	0	0
Alumina Powder	1.000	0.891	0	0

Summary of γ coefficients for three target media

EVALUATION of γ

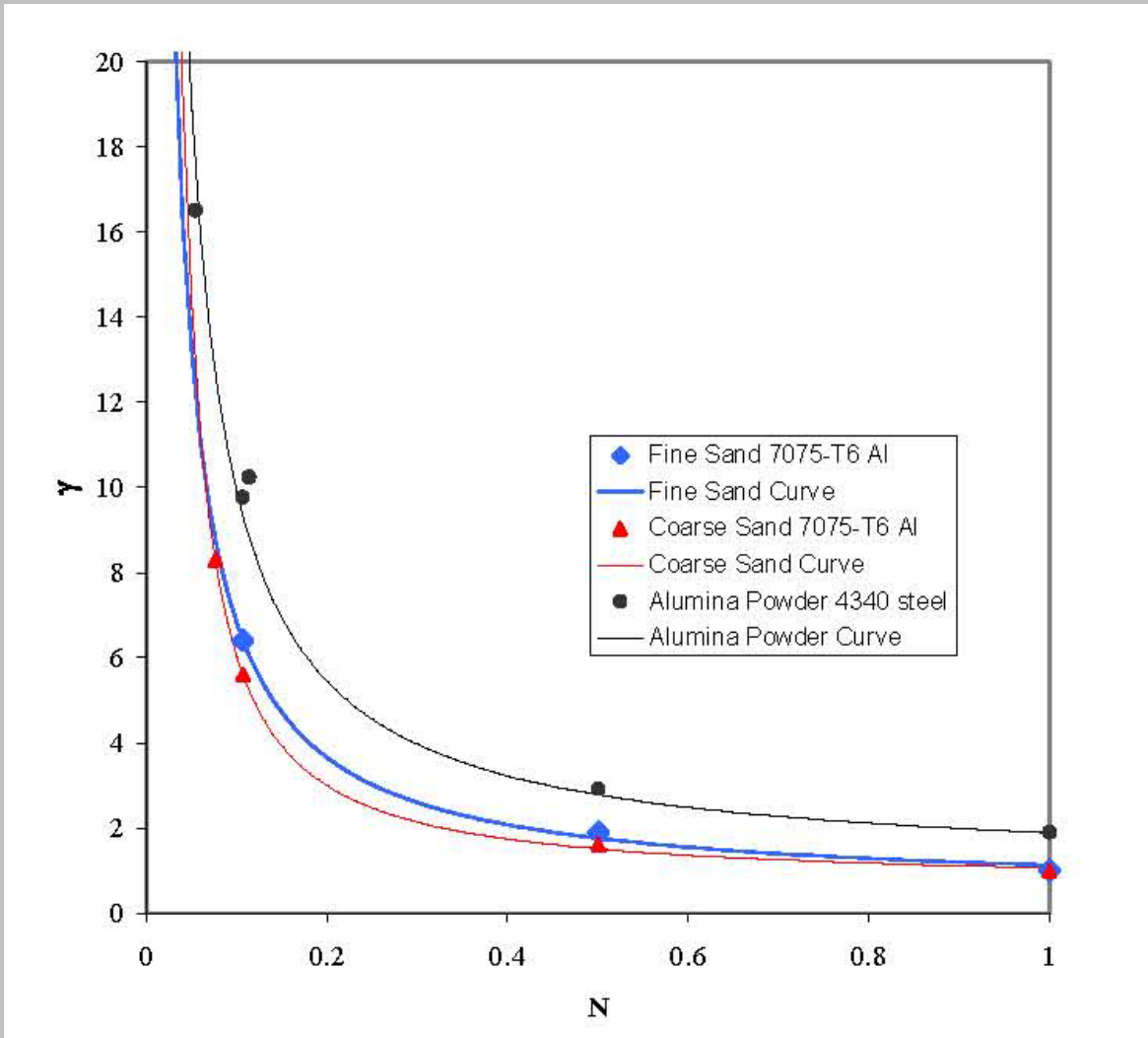

Graph of γ vs. N for each target medium

EVALUATION of γ

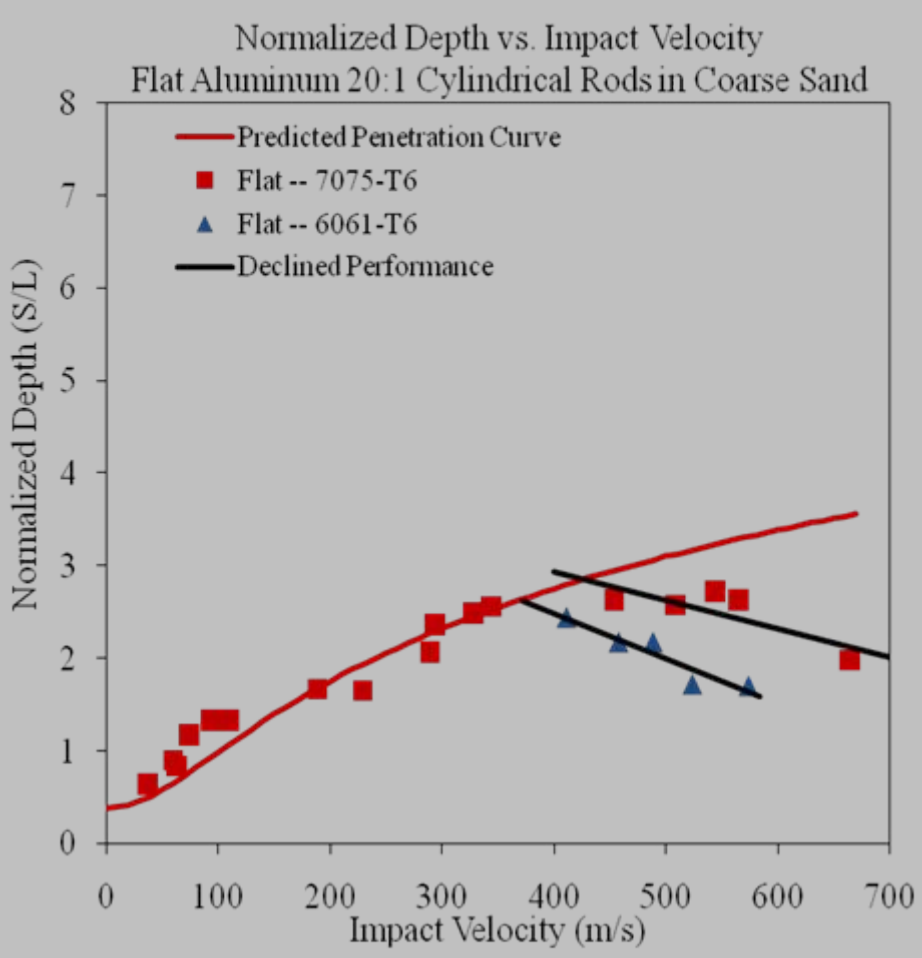

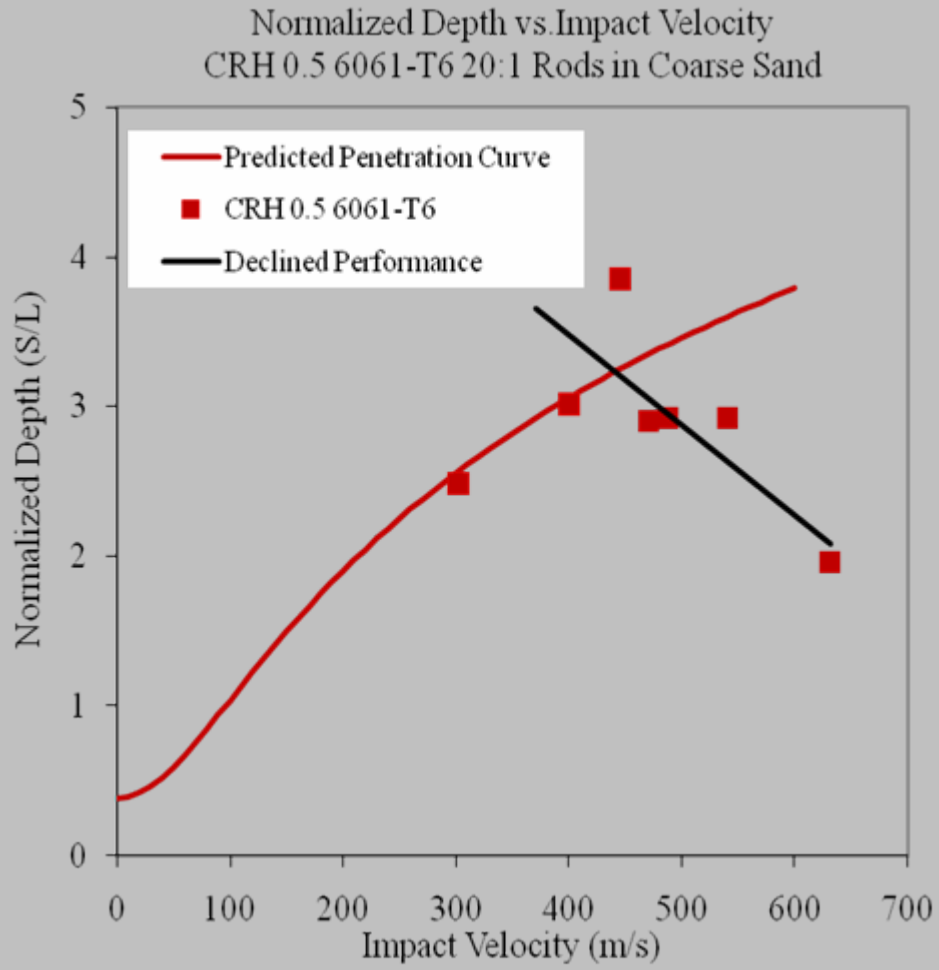

EVALUATION of γ

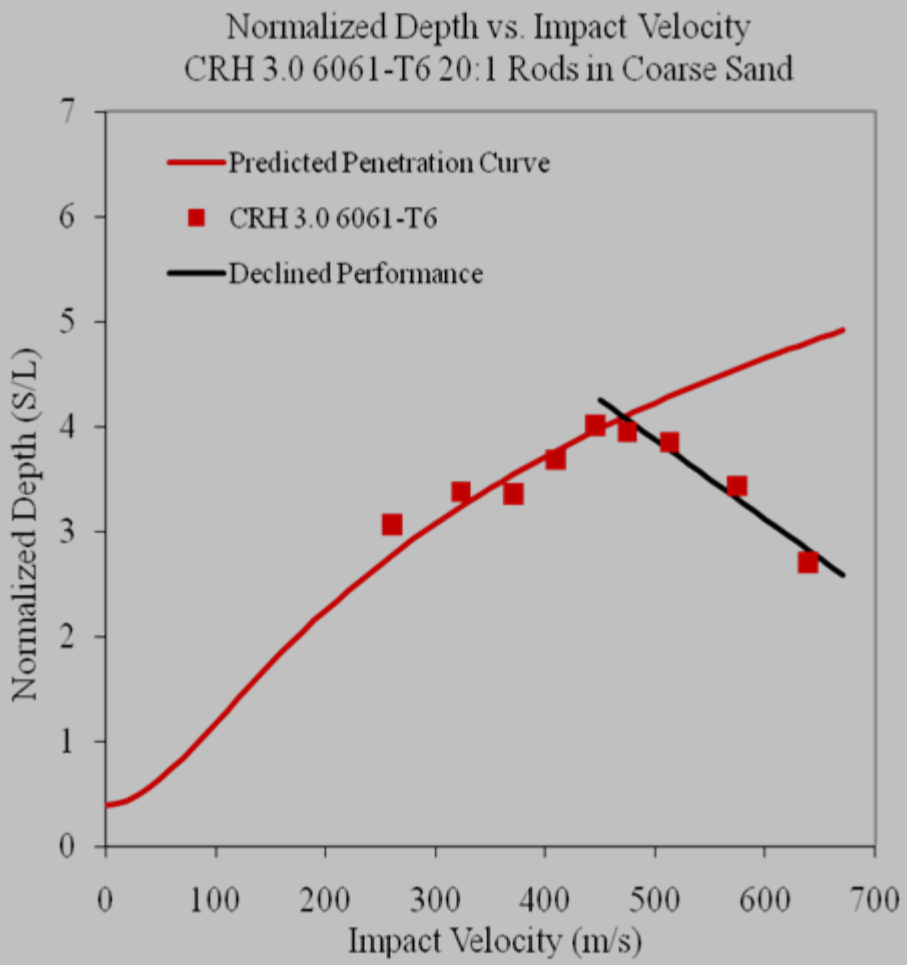

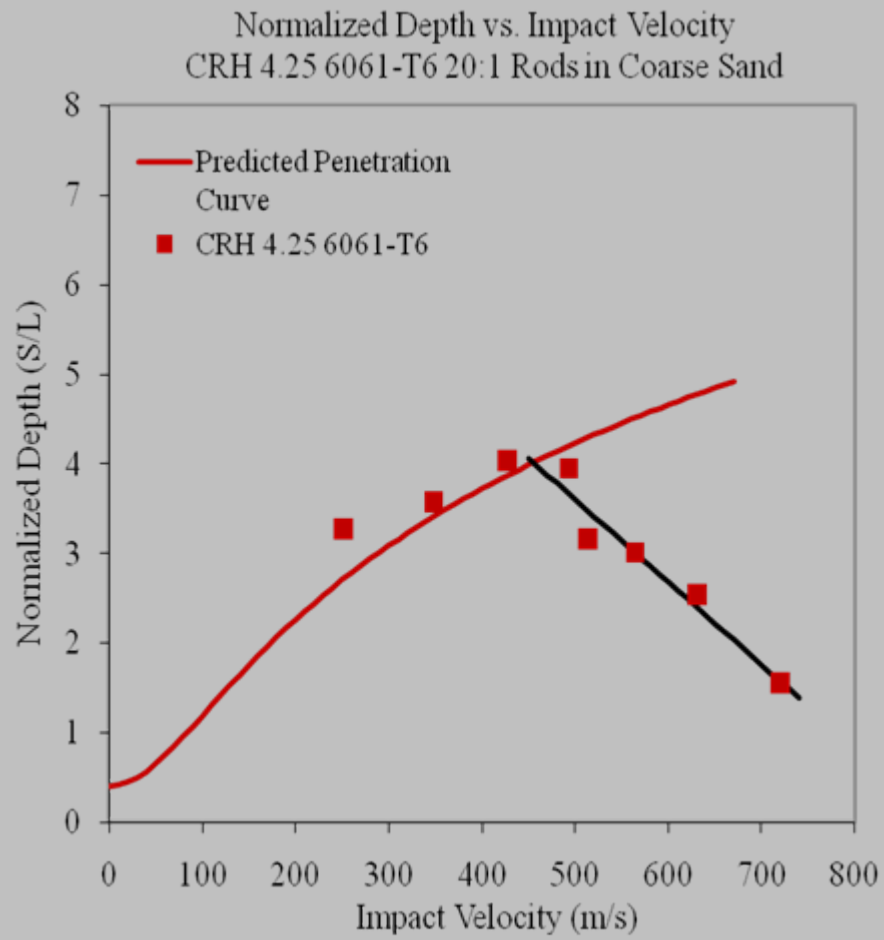

Formulation and Solution of the Problem

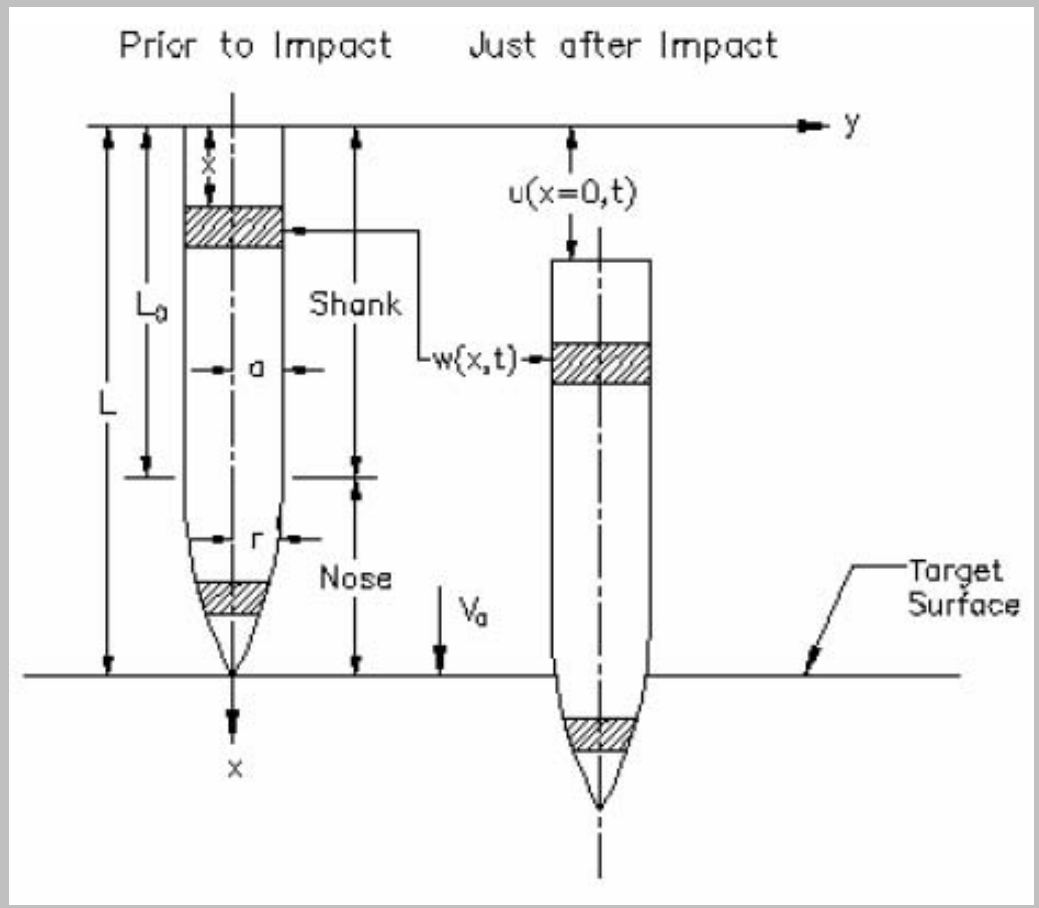

The Lagrangian coordinate system

Formulation and Solution of the Problem

$$\rho \pi r^2 \frac{\partial^2 u}{\partial t^2} = \frac{\partial P}{\partial x}$$

$$\rho \pi r^2 \frac{\partial^2 w}{\partial t^2} = \frac{\partial Q}{\partial x}$$

$$\rho \pi r^2 \frac{\partial^2 w}{\partial t^2} + \frac{\partial^2}{\partial x^2}\left(EI \frac{\partial^2 w}{\partial x^2} \right) - \frac{\partial}{\partial x}\left(P \frac{\partial w}{\partial x} \right) = 0$$

Longitudinal Force

$$m\dot{v}_G = -F(v_G(t))$$

$$\frac{\partial^2 u}{\partial t^2} = \dot{v}_G$$

$$\frac{\partial P}{\partial x} = \rho \pi r^2 \dot{v}_G \qquad 0 < x < L$$

Longitudinal Force

$$P(x,t) = \rho\pi a^2 \dot{v}_G x$$

$$0 < x < L_0$$

$$P(L_0,t) = \rho\pi a^2 \dot{v}_G L_0$$

$$P(x,t) = \rho\pi a^2 \dot{v}_G L_0 + \rho\pi \dot{v}_G \int_{L_0}^{x} r^2(x)dx$$

$$L_0 < x < L$$

Lateral Motion

$$\rho\pi a^2 \frac{\partial^2 w}{\partial t^2} + \frac{\partial^2}{\partial x^2}\left(EI \frac{\partial^2 w}{\partial x^2} \right) - \frac{\partial}{\partial x}\left(\rho\pi a^2 \dot{v}_G x \frac{\partial w}{\partial x} \right) = 0$$

$$0 < x < L_0$$

$$\rho\pi r^2 \frac{\partial^2 w}{\partial t^2} + \frac{\partial^2}{\partial x^2}\left(EI \frac{\partial^2 w}{\partial x^2} \right) - \frac{\partial}{\partial x}\left(\rho\pi \dot{v}_G (a^2 L_0 + \int_{L_0}^{x} r^2(x)dx) \frac{\partial w}{\partial x} \right) = 0$$

$$L_0 < x < L$$

Homogeneous Boundary Conditions

$$\frac{\partial^2 w}{\partial x^2}(0,t) = \frac{\partial^3 w}{\partial x^3}(0,t) = 0$$

$$w(L,t) = 0$$

$$\frac{\partial^2 w}{\partial x^2}(L,t) = 0$$

Dimensionless Variables

$$\xi = \frac{x}{L} \qquad \beta = \frac{r(x)}{a} \qquad z = \frac{w}{a} \qquad \tau = \frac{v_0 t}{L}$$

$$\frac{EI}{\rho \pi a^2 v_0^2 L^2} \frac{\partial^4 z}{\partial \xi^2} + \frac{\partial^2 z}{\partial \tau^2} - \frac{L \dot{v}_G}{v_0^2} \frac{\partial}{\partial \xi} \left(\xi \frac{\partial z}{\partial \xi} \right) = 0$$

$$0 < \xi < \xi_0$$

$$\frac{Ea^2}{\rho \pi v_0^2 L^2 \beta^2} \frac{\partial^2}{\partial \xi^2} \left(\frac{I}{a^4} \frac{\partial^2 z}{\partial \xi^2} \right) + \frac{\partial^2 z}{\partial \tau^2} - \frac{L \dot{v}_G}{\beta^2 v_0^2} \frac{\partial}{\partial \xi} \left(\left(\xi_0 + \int_{\xi_0}^{\xi} \beta^2 d\xi \right) \frac{\partial z}{\partial \xi} \right) = 0$$

$$\xi_0 < \xi < 1$$

Deceleration Approximation

$$\dot{v}_G = -\frac{F}{m} \cong -\frac{\pi a^2 \gamma \rho_t N v_0^2}{m}$$

Separation of Variables

$$z = \Phi(\xi)T(\tau) \qquad \ddot{T} + \omega T = 0$$

$$\frac{EI}{\rho\pi a^2 v_0^2 L^2}\frac{d^4\Phi}{d\xi^4} - \omega\Phi + \frac{L\pi a^2\gamma\rho_t N}{m}\frac{d}{d\xi}\left(\xi\frac{d\Phi}{d\xi}\right) = 0$$

$$0 < \xi < \xi_0$$

$$\frac{Ea^2}{\rho\pi v_0^2 L^2\beta^2}\frac{d^2}{d\xi^2}\left(\frac{I}{a^4}\frac{d^2\Phi}{d\xi^2}\right) - \omega\Phi + \frac{L\pi a^2\gamma\rho_t N}{m\beta^2}\frac{d}{d\xi}\left(\left(\xi_0 + \int_{\xi_0}^{\xi}\beta^2 d\xi\right)\frac{d\Phi}{d\xi}\right) = 0$$

$$\xi_0 < \xi < 1$$

Boundary Conditions

$$\frac{d^2\Phi}{d\xi^2}(0) = \frac{d^3\Phi}{d\xi^3}(0) = 0$$

$$\Phi(1) = \frac{d^2\Phi}{d\xi^2}(1) = 0$$

Separation of Variables

$$\lambda \frac{d^4\Phi}{d\xi^4} - \omega\Phi + \eta \frac{d}{d\xi}\left(\xi \frac{d\Phi}{d\xi}\right) = 0$$

$$0 < \xi < \xi_0$$

$$\lambda \frac{d^2}{d\xi^2}\left(\beta^4 \frac{d^2\Phi}{d\xi^2}\right) - \omega\beta^2\Phi + \eta \frac{d}{d\xi}\left(\left(\xi_0 + \int_{\xi_0}^{\xi} \beta^2 d\xi\right)\frac{d\Phi}{d\xi}\right) = 0$$

$$\xi_0 < \xi < 1$$

$$\lambda = \frac{EI_S}{\rho\pi a^2 v_0^2 L^2}$$

$$\eta = \frac{\pi L a^2 \gamma \rho_t N}{m}$$

Orthogonality of the Eigenfunctions

Consider, for simplicity, the case for a flat-ended cylinder.

$$\lambda \frac{d^4 \Phi_n}{d\xi^4} + \eta \frac{d}{d\xi}\left(\xi \frac{d\Phi_n}{d\xi} \right) - \omega_n \Phi_n = 0$$

It is not difficult to show that

$$\int_0^1 \Phi_m \Phi_n d\xi = 0 \qquad m \neq n$$

$$\omega_n = \frac{\lambda \int_0^1 \left(\frac{d^2 \Phi_n}{d\xi^2} \right)^2 d\xi - \eta \int_0^1 \xi \left(\frac{d\Phi_n}{d\xi} \right)^2 d\xi}{\int_0^1 \Phi_n^2 d\xi}$$

Orthogonality of the Eigenfunctions

Consider

$$\omega = \frac{\lambda \int_0^1 \left(\frac{d^2\Phi}{d\xi^2} \right)^2 d\xi - \eta \int_0^1 \xi \left(\frac{d\Phi}{d\xi} \right)^2 d\xi}{\int_0^1 \Phi^2 d\xi}$$

$$\Phi = k_1\Phi_1 + k_2\Phi_2 + \ldots$$

Orthogonality of the Eigenfunctions

$$\omega = \frac{\omega_1 k_1^2 \int_0^1 \Phi_1^2 d\xi + \omega_2 k_2^2 \int_0^1 \Phi_2^2 d\xi + \ldots + \omega_n k_n^2 \int_0^1 \Phi_n^2 d\xi + \ldots}{k_1^2 \int_0^1 \Phi_1^2 d\xi + k_2^2 \int_0^1 \Phi_2^2 d\xi + \ldots + k_n^2 \int_0^1 \Phi_n^2 d\xi + \ldots}$$

The Stationary Values achieved by this quotient are the Eigenvalues $\omega_1, \omega_2, \ldots$

Ogive Noses

$$\omega_n = \frac{\lambda\left[\int_0^{\xi_0}\left(\frac{d^2\Phi_n}{d\xi^2}\right)^2 d\xi + \int_0^1 \beta^4\left(\frac{d^2\Phi_n}{d\xi^2}\right)^2 d\xi\right] - \eta\left[\int_0^{\xi_0}\xi\left(\frac{d\Phi_n}{d\xi}\right)^2 d\xi + \int_{\xi_0}^1\left(\xi_0 + \int_{\psi_0}^{\xi}\beta^2 d\xi\right)\left(\frac{d\Phi_n}{d\xi}\right)^2 d\xi\right]}{\int_0^{\xi_0}\Phi_n^2 d\xi + \int_{\xi_0}^1 \beta^2\Phi_n^2 d\xi}$$

$$\beta'(\xi_0) = 0$$

Stability Criterion

$$\omega_1 = \frac{\lambda\left[\int_0^{\xi_0}\left(\frac{d^2\Phi_1}{d\xi^2}\right)^2 d\xi + \int_{\xi_0}^{1}\beta^4\left(\frac{d^2\Phi_1}{d\xi^2}\right)^2 d\xi\right] - \eta\left[\int_0^{\xi_0}\xi\left(\frac{d\Phi_1}{d\xi}\right)^2 d\xi + \int_{\xi_0}^{1}\left(\xi_0 + \int_{\xi_0}^{\xi}\beta^2 d\xi\right)\left(\frac{d\Phi_1}{d\xi}\right)^2 d\xi\right]}{\int_0^{\xi_0}\Phi_1^2 d\xi + \int_{\xi_0}^{1}\beta^2\Phi_1^2 d\xi} > 0$$

where ω_1 is the lowest eigenvalue and Φ_1 is the corresponding eigenfunction

Trial Functions

$$\Phi = 1 - \frac{5}{2}\xi^4 + \frac{3}{2}\xi^5 + \left(\xi - \frac{5}{2}\xi^4 + \frac{3}{2}\xi^5\right)C_1 + \left(1 - \frac{20}{3}\xi^4 + 9\xi^5 - \frac{10}{3}\xi^6\right)C_2$$

Choose C_1 and C_2 so that a minimum in the quotient is achieved.

Results

Critical Velocity of 20:1 6061 T-6 Aluminum into Course Foundry Sand				
	Flat	CRH 0.5	CRH 3.0	CRH 4.25
Two Constant Estimate	384.03 (m/s)	405 (m/s)	452 (m/s)	450.2 (m/s)
Experimental	375 (m/s)	435 (m/s)	475 (m/s)	445 (m/s)

Critical Velocity Comparisons

Critical Velocity of 20:1 6061 T-6 Aluminum into Course Foundry Sand				
	Flat	CRH 0.5	CRH 3.0	CRH 4.25
One Constant Estimate	495.25 (m/s)	522.32 (m/s)	589.265 (m/s)	613.934 (m/s)
Two Constant Estimate	384.03 (m/s)	405 (m/s)	452 (m/s)	450.2 (m/s)
Torres Estimate	406 (m/s)	421 (m/s)	472 (m/s)	468 (m/s)

Theory Comparisons

Results

7075- T6 Aluminum CRH 12 into Course Foundry Sand		
	8:1	12:1
One Constant Estimate	819.13 (m/s)	822.76 (m/s)
Two Constant Estimate	679.17 (m/s)	683.14 (m/s)
Torres Estimate	680 (m/s)	680 (m/s)
Experimental Result	700 (m/s)	690 (m/s)

More Theory Comparisons

Results

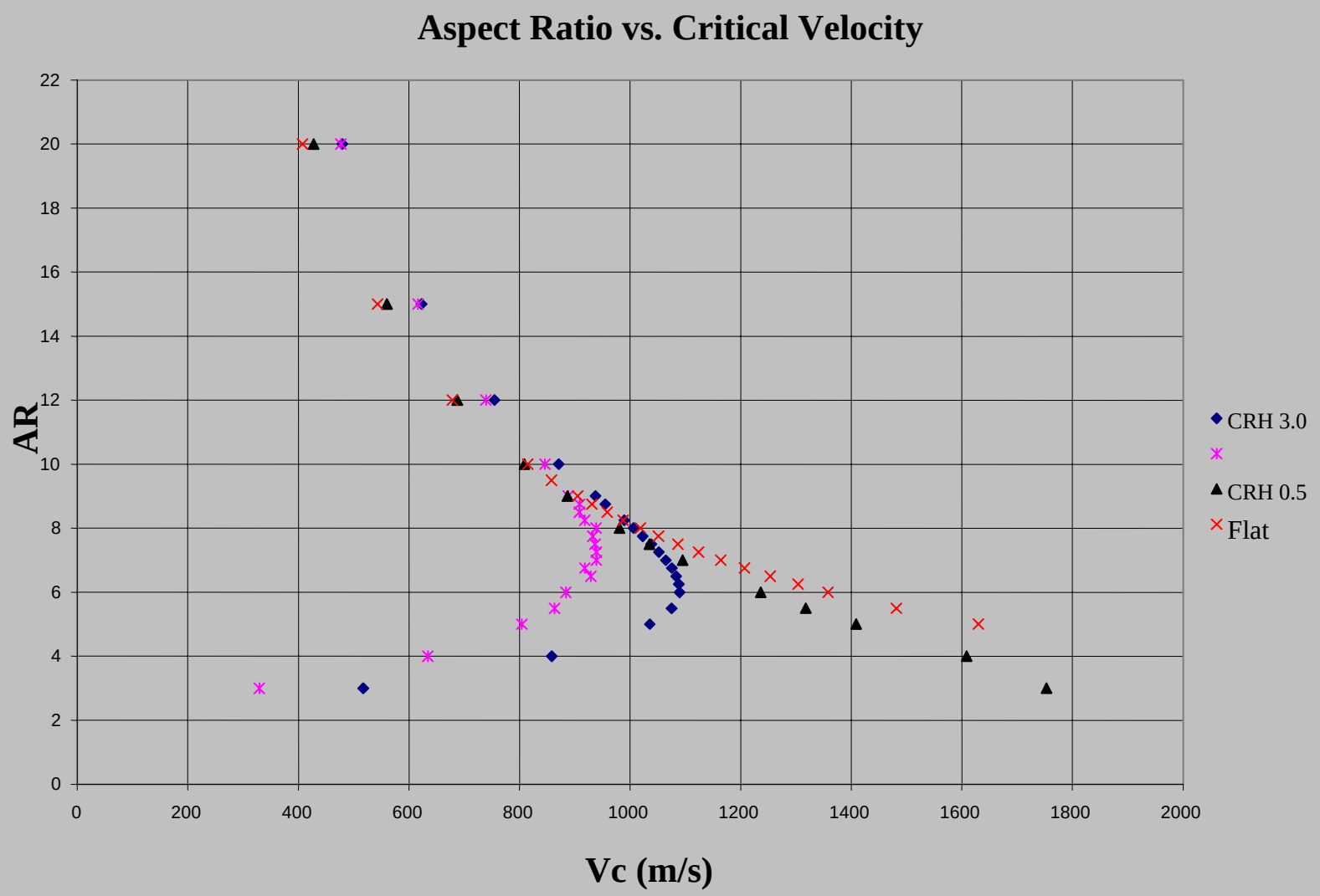
Aspect Ratio vs. Critical Velocity
AR
Vc (m/s)
0
2
4
6
8
10
12
14
16
18
20
22
0
200
400
600
800
1000
1200
1400
1600
1800
2000
CRH 3.0
CRH 0.5
Flat

Results

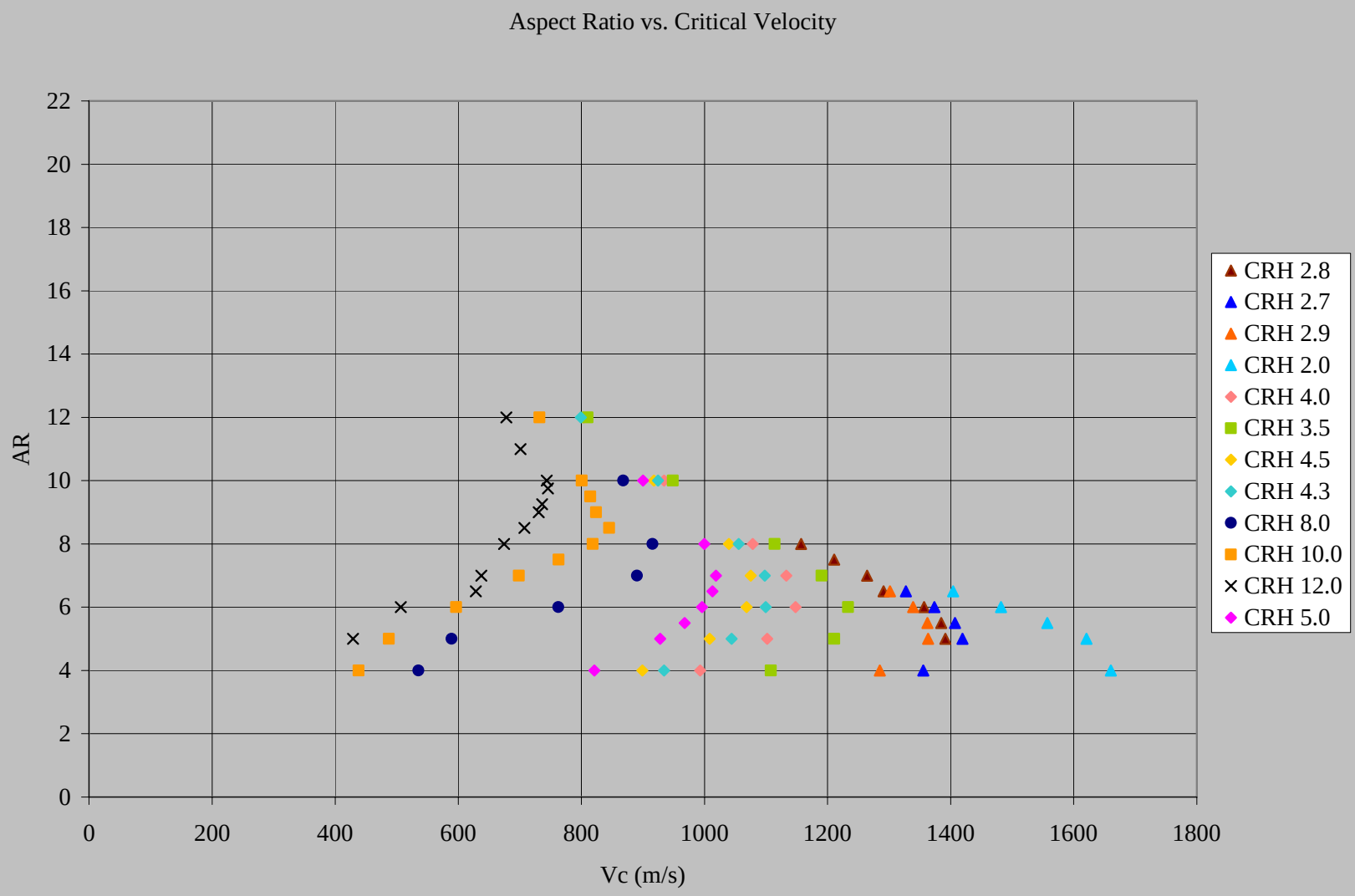
Aspect Ratio vs. Critical Velocity
AR
Vc (m/s)
0
2
4
6
8
10
12
14
16
18
20
22
0
200
400
600
800
1000
1200
1400
1600
1800
CRH 2.8
CRH 2.7
CRH 2.9
CRH 2.0
CRH 4.0
CRH 3.5
CRH 4.5
CRH 4.3
CRH 8.0
CRH 10.0
CRH 12.0
CRH 5.0

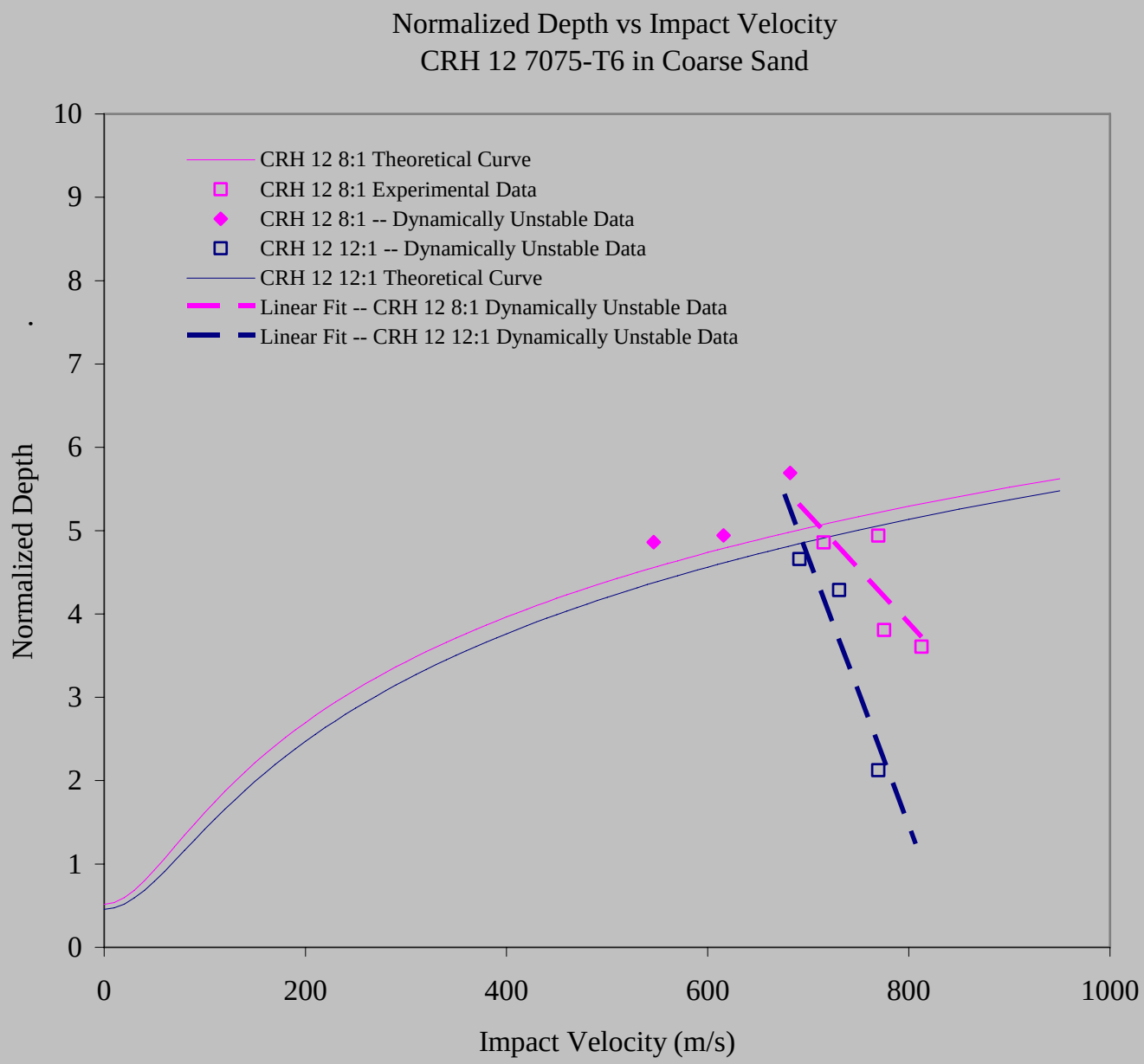
Normalized Depth vs Impact Velocity
CRH 12 7075-T6 in Coarse Sand
CRH 12 8:1 Theoretical Curve
CRH 12 8:1 Experimental Data
CRH 12 8:1 -- Dynamically Unstable Data
CRH 12 12:1 -- Dynamically Unstable Data
CRH 12 12:1 Theoretical Curve
Linear Fit -- CRH 12 8:1 Dynamically Unstable Data
Linear Fit -- CRH 12 12:1 Dynamically Unstable Data
Normalized Depth
Impact Velocity (m/s)
0
1
2
3
4
5
6
7
8
9
10
0
200
400
600
800
1000

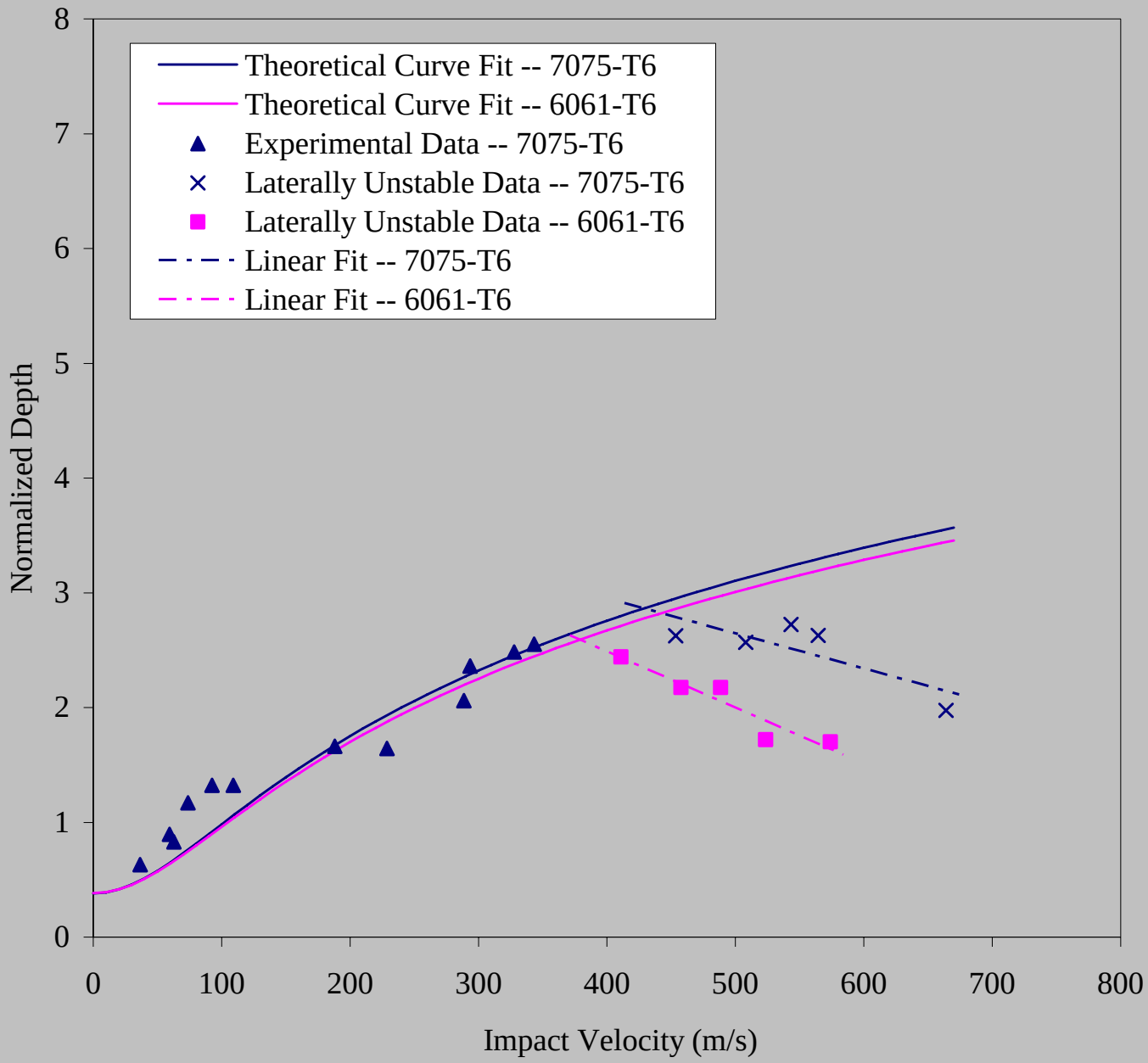
Normalized Depth vs. Impact Velocity
7075-T6 and 6061-T6 20:1 Cylindrical Rods in Coarse Sand
Theoretical Curve Fit -- 7075-T6
Theoretical Curve Fit -- 6061-T6
Experimental Data -- 7075-T6
Laterally Unstable Data -- 7075-T6
Laterally Unstable Data -- 6061-T6
Linear Fit -- 7075-T6
Linear Fit -- 6061-T6
Normalized Depth
0
1
2
3
4
5
6
7
8
0
100
200
300
400
500
600
700
800
Impact Velocity (m/s)

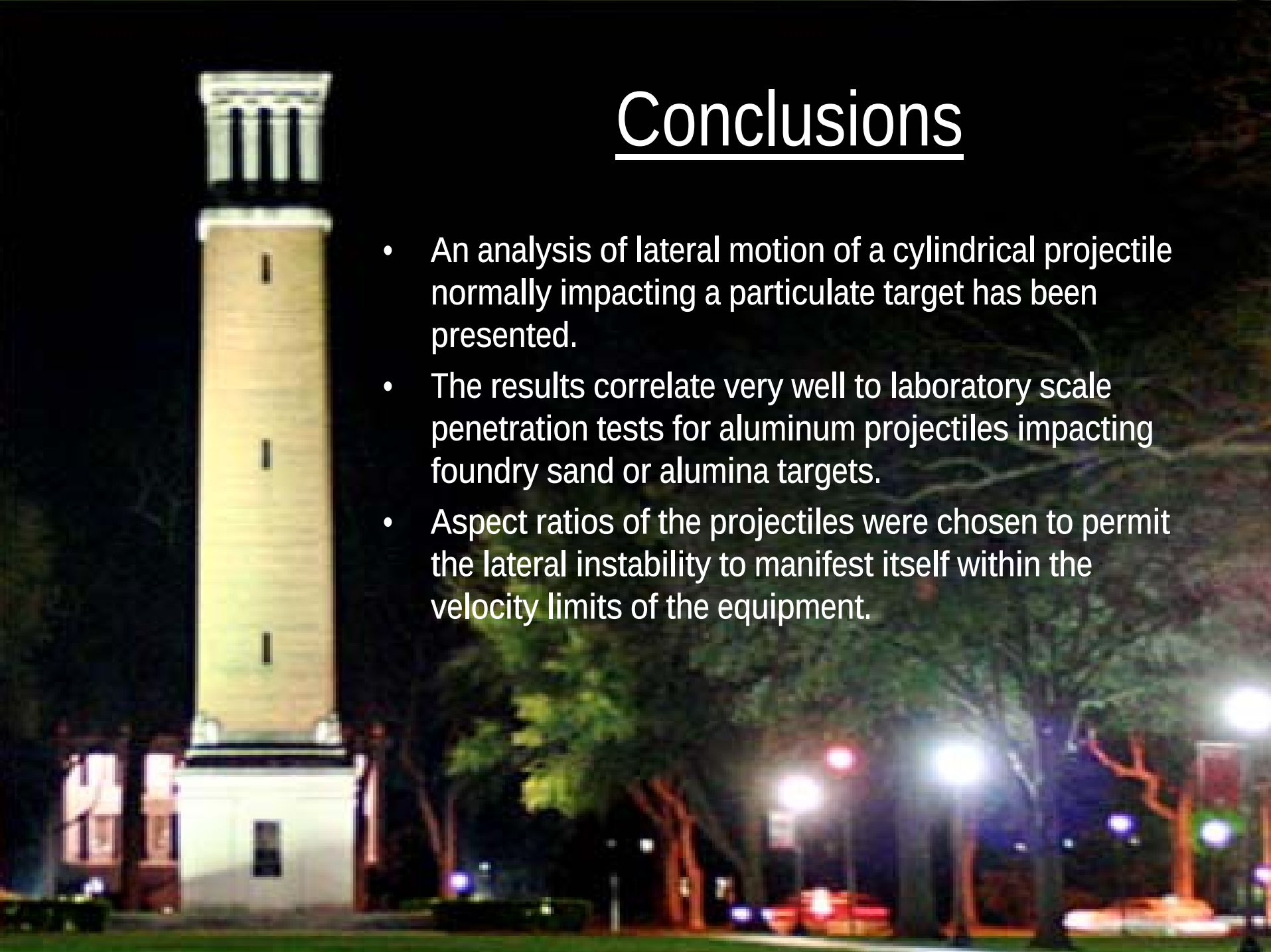

Conclusions

- An analysis of lateral motion of a cylindrical projectile normally impacting a particulate target has been presented.
- The results correlate very well to laboratory scale penetration tests for aluminum projectiles impacting foundry sand or alumina targets.
- Aspect ratios of the projectiles were chosen to permit the lateral instability to manifest itself within the velocity limits of the equipment.

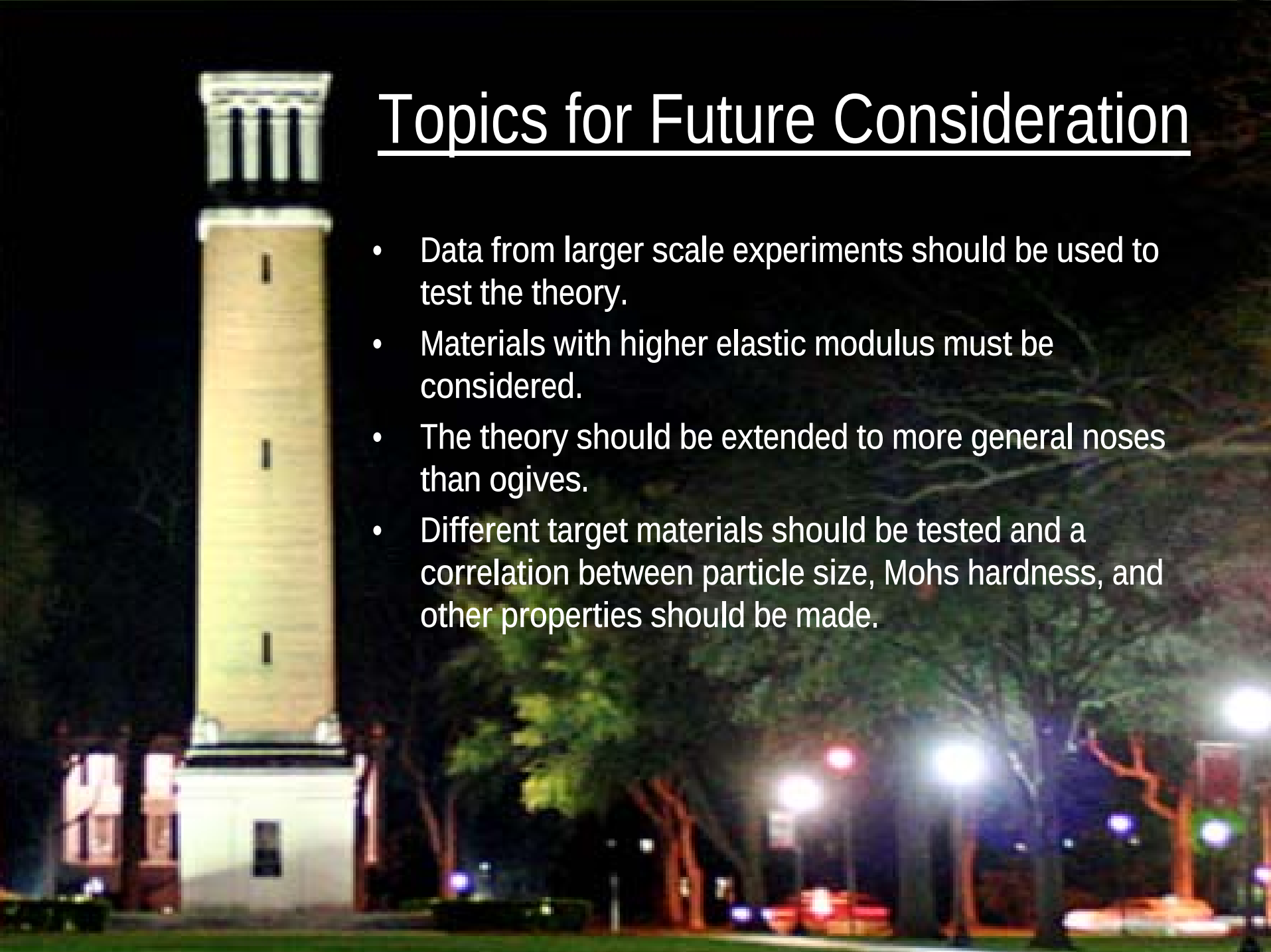

Topics for Future Consideration

- Data from larger scale experiments should be used to test the theory.
- Materials with higher elastic modulus must be considered.
- The theory should be extended to more general noses than ogives.
- Different target materials should be tested and a correlation between particle size, Mohs hardness, and other properties should be made.

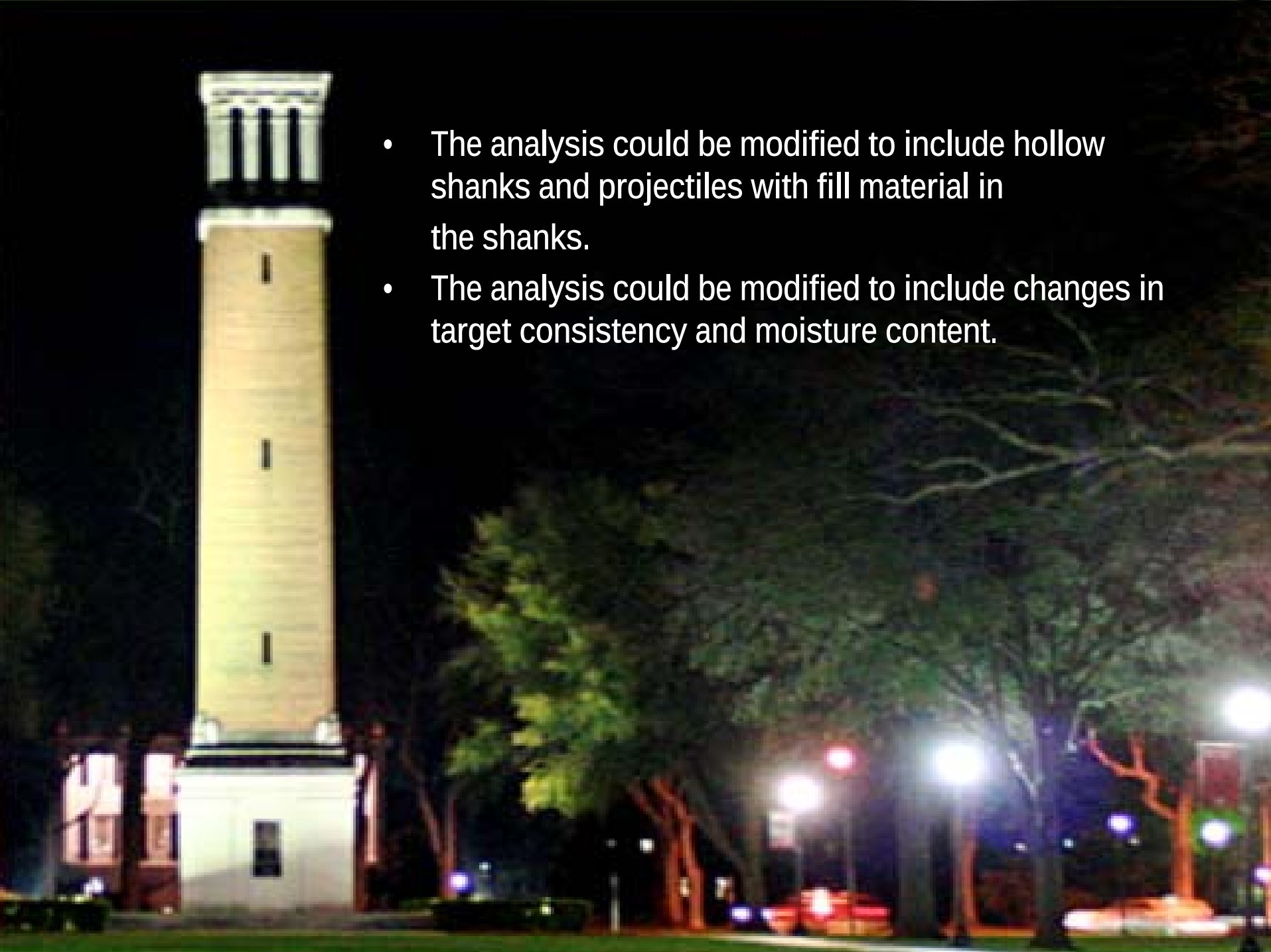

- The analysis could be modified to include hollow shanks and projectiles with fill material in the shanks.
- The analysis could be modified to include changes in target consistency and moisture content.